Aerodynamic admittance functions of streamlined bodies: the indicial approach by CWE

L. Bruno[a], F. Tubino [b], G. Solari [b]

[a] Politecnico di Torino, Dipartimento di Ingegneria Strutturale e Geotecnica, Torino
[b] Università di Genova, Dipartimento di Ingegneria Strutturale e Geotecnica, Genova

ABSTRACT

This paper proposes a method to determine the aerodynamic admittance function of 2-dimensional cylinders by means of a modified indicial approach adapted to a Navier-Stokes solver. The method is based on the simulation of a smoothed-edge gust passing the cylinder and on the evaluation of the transient forces arising on the obstacle. An application to a thin plate is proposed. Firstly, the numerical parameters of the model are optimised by simulating two elementary flow conditions: the gust propagation in a free stream and the steady flow around the plate. Then, both the gust and the plate are introduced in the same computational model. The computed aerodynamic admittance function is compared with the one provided in closed form by Sears in the frame of the thin airfoil theory.

KEYWORDS: Aerodynamic admittance function, Computational Wind Engineering, Indicial function.

1. INTRODUCTION

The aerodynamic admittance function is intended here as the transfer function of the linear aerodynamic operator mapping the fluctuations of the incident flow on a body into the force components arising on the body itself. The evaluation of this function is useful to predict the aerodynamic response of obstacles in a number of applications, for instance a wing flying into a blast gust or encountering turbulence, a bridge deck lying in the turbulent atmospheric boundary layer or a car running across wind gusts near the ground.

Several experimental approaches have been proposed within this scope for bridge engineering applications during the last decade (Larose 1999, Cigada *et al* 2002). On the contrary, despite the continuous and relevant increase of computing facilities, the computational approach did not represent up to now a reliable alternative to the experimental tests. That is mostly due to the difficulties in simply transferring the experimental approaches to the computational field by the numerical simulation of the wind tunnel test. The numerical generation of imposed inflow turbulence analogously to the incoming turbulence obtained in wind tunnel tests (Larose 1999) is still a matter of research (Murakami *et al* 1999). Moreover, the simulation of the stationary response of the body to the turbulent fluctuations should be computationally very burdensome. Analogously, it would be time consuming imposing harmonic variations of the velocity components at boundary inlet and performing a numerical simulation for each circular frequency of interest (Cigada *et al* 2002).

An effective reduction of the time extension of the numerical simulation can be achieved evaluating aerodynamic admittance functions through the indicial approach (Von Karman and Sears 1938). The method has been introduced in literature for the assessment of the aerodynamic and aeroelastic forces acting on a thin airfoil, in non uniform motion and potential flow (Fung 1993). Generally

speaking, the indicial approach consists in the determination of the generalised forces (drag, lift and moment) arising on a body as a consequence of a step variation of the motion of the body (Wagner problem) or due to its transition through a step-variation of the flow field (Küssner problem). Thanks to the hypothesis of linearity of the aerodynamic operator, the force acting on the body due to any temporal variation of a generic parameter can be evaluated from the step response function through a Duhamel integral. The aerodynamic admittance functions, introduced within a frequency domain representation of the force components, can be estimated from the indicial functions through Fourier transform operations.

The computational estimation of aerodynamic admittance functions by the indicial approach has been firstly proposed by Turbelin (2000). According to the authors of the present paper, some unsolved problems still remain in the numerical application of the indicial approach.

First of all, the variation in time and space of the input variable according to a Heaviside function can't be imposed because of the finite nature of the discretization.

Secondly, every abrupt variation of the input variable involves very high values of the variable derivatives in space and time. Hence, numerical oscillations affecting the transient solution of interest can arise in the solution of the Navier-Stokes equations. The methods to be applied for the computational generation of an input arbitrary smoothed ramp function have been analysed in the aeronautical field with reference to variations of the velocity components of the body (Wagner problem) in compressible flow (Ballhaus and Goorjian 1978, Lesieutre *et al* 1994, Parameswaran and Baeder 1997).

Thirdly, the generation of an arbitrary fluctuation of the input variable does not apply to the undisturbed velocity field components because the physical evolution of the gust can be violated.

Finally, the numerical investigation of aerodynamic phenomena involving high gradients of some variables requires very fine characteristics of the computational model as far as concerns the quality of the grid and the accuracy of the discretization schemes both in time and in space (Tamura 1990).

In order to overcome the above mentioned difficulties, this paper proposes a procedure for the computational evaluation of aerodynamic admittance functions by means of a modified indicial approach.

The propagation of a gust in a free stream is first simulated in order to perform a preliminary sensitivity study to evaluate the dispersive and diffusive effects introduced into the solution by the numerical parameters of the model (grid density, time step, schemes for the spatial and time discretization). The tuning of the parameters is verified with reference to the analytical solution of the heat diffusion equation (Batchelor 1967).

In what follows the proposed methodology is applied to a thin plate for various flow models. The simulation of the aerodynamic behaviour of the plate in steady viscous flow is preliminarily accomplished and validated with respect to the well known Blasius' solution. The results obtained subsequently to the gust generation show the relationship among the gust propagation, the transient flow field around the obstacle, the evolution of the aerodynamic force and the aerodynamic admittance function. Hence, the numerically evaluated aerodynamic admittance function is compared with the well known Sears function (Von Karman and Sears 1938) and a good agreement is found, validating the proposed procedure.

The extension of the approach to bluff bridge deck sections is discussed in a companion paper (Bruno *et al* 2004).

2. AERODYNAMIC ADMITTANCE FUNCTION AND INDICIAL APPROACH

Let us consider a 2-dimensional turbulent flow field, modelled as a mean wind velocity U and two fluctuating components $u(t)$ in the mean wind velocity direction (x) and $w(t)$ in the vertical direction (z). A fixed body immersed in this flow field is subjected to a set of forces: a drag force $F_x(t)$ in the longitudinal direction, a lift force $F_z(t)$ in the vertical direction and a torsional moment $M(t)$ (Figure 1a). The fluctuating components of these forces are commonly called buffeting forces.

The lift force induced on a thin airfoil is commonly expressed, in the frequency domain, as a function of the vertical turbulence component as follows:

$$F_z(\omega) = \frac{1}{2}\rho U^2 B c'_L \chi(\omega) w(\omega) \tag{1}$$

where $F_z(\omega)$ and $w(\omega)$ represent, respectively, the Fourier transforms of the lift force and of the vertical turbulence component, ρ is the air density, B is the chord of the airfoil, c'_L is the derivative of the lift coefficient with respect to the angle of attack and $\chi(\omega)$ is the aerodynamic admittance function. Hence, the body can be interpreted as a linear aerodynamic operator (Figure 1b), mapping the incident flow field into the force component (Fung 1993).

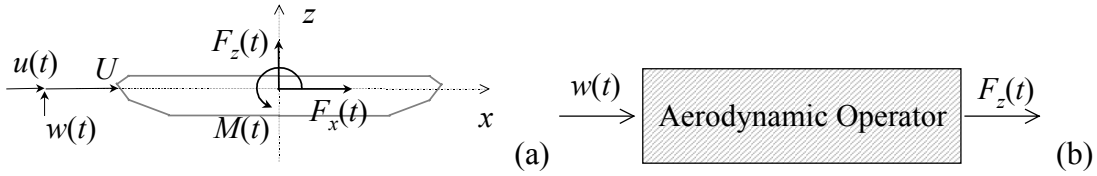

Figure 1: Buffeting forces on 2-dimensional cylinders.

The time domain counterpart of Eq. (1) can be written as follows:

$$F_z(t) = \frac{1}{2}\rho U^2 B c'_L \int_0^t w(\tau) h(t-\tau)\,\mathrm{d}\tau \tag{2}$$

where $h(t)$ is the impulse response function of the aerodynamic operator, i.e. the lift force on the body due to an elementary impulse variation of the vertical turbulence component; it is related to the aerodynamic admittance function $\chi(\omega)$ by a Fourier transform operation: $\chi(\omega)=F[h(t)]$, F being the Fourier transform operator.

Alternatively, Eq. (2) can be written as follows:

$$F_z(t) = \frac{1}{2}\rho U^2 B c'_L \left[w(0) g(t) + \int_0^t \dot{w}(\tau) g(t-\tau)\,\mathrm{d}\tau \right] \tag{3}$$

where $g(t)$ is the step response function: it is the time derivative of the impulse response function $h(t)=\mathrm{d}g(t)/\mathrm{d}t$.

The functions $h(t)$, $\chi(\omega)$ and $g(t)$ are known in closed form for a thin airfoil under the hypothesis of potential flow and the latter ones are respectively called Sears function and Küssner function (Von Karman and Sears 1938, Fung 1993).

The aerodynamic admittance function can be evaluated from the lift due to a generic time history of the vertical velocity by Eq. (1). If the time histories of the vertical velocity $w(t)$ or of the lift force $F_z(t)$ are not absolutely integrable, their Fourier transform cannot be defined and Eq. (1) cannot be applied. Such difficulty can be overcome in virtue of the hypothesis of linearity of the aerodynamic operator that extends the relationship linking the vertical velocity component $w(t)$ and the lift force $F_z(t)$ to their time derivatives $\dot{w}(t)$ and $\dot{F}_z(t)$. Thus, the aerodynamic admittance function can be determined from the following Equation:

$$\chi(\omega) = \frac{\dot{F}_z(\omega)}{\frac{1}{2}\rho U^2 b c'_L \dot{W}(\omega)} \tag{4}$$

where $\dot{F}_z(\omega)$ and $\dot{W}(\omega)$ represent the Fourier transform of $\dot{w}(t)$ and $\dot{F}_z(t)$, respectively.

3. VALIDATION OF THE COMPUTATIONAL TOOL

Computations were carried out using the FLUENT 6.1 code, based on the Finite Volume Method (FVM). Being the description of the computational method out of the scope of this paper, only relevant aspects are explained in the following if required to better comment the obtained results.

The computational simulation of the gust response of the thin airfoil calls for a preliminary assessment of the accuracy of the results of the computational tool for elementary flow conditions.
At first, the correct simulation of the gust propagation in absence of the obstacle is tested. This study allows to determine the discretization requirements in time and space in order to guarantee the efficient simulation of the propagation of the gust. Secondly, the steady-state viscous flow at null incidence around the thin airfoil is simulated in order to evaluate the accuracy of the computational simulation of the attached laminar boundary layer surrounding the wall.

3.1. Gust propagation in a free stream

The evolution of an initially sharp-edge gust can be predicted in closed form.
Let us consider a 2-dimensional laminar viscous flow characterised at time $t < t_0$ by a horizontal component $U=\bar{U}$ and a null vertical component $W=0$; at time t_0 a discontinuous variation of magnitude $\bar{W}$ of the vertical component W of the velocity field is imposed for each abscissa of the domain $x < x_0$:

$$\begin{cases} W(x;t)=0 & t<t_0 \ \ \forall x \ \ \forall z \\ W(x;t)=\bar{W} & t=t_0 \ \ x<x_0 \ \ \forall z \end{cases} \tag{5}$$

Let us introduce a new reference system x^*y^* moving along the x direction with speed $\bar{U}$ and two new variables U^* and W^* defined as follows:

$$\begin{cases} x^*=x-\bar{U}t \\ z^*=z \end{cases} \qquad \begin{cases} U^*=U-\bar{U}=0 \\ W^*=W \end{cases} \tag{6}$$

Moreover, let us assume that the pressure and the velocity in the x-direction U are constant in time and space. Under the above mentioned hypothesis the Navier Stokes Equations (NSE) governing the flow can be simplified and reduced to the simple diffusion problem:

$$\frac{\partial W^*}{\partial t}=\nu\cdot\left(\frac{\partial^2 W^*}{\partial z^{*2}}+\frac{\partial^2 W^*}{\partial x^{*2}}\right) \qquad \begin{cases} W^*(x^*;0)=-\dfrac{\bar{W}}{2} & x^*<x_0 \\ W^*(x^*;0)=+\dfrac{\bar{W}}{2} & x^*>x_0 \end{cases} \tag{7}$$

The solution of Eq. (7) is available in closed form in accordance with the heat diffusion equation (Batchelor 1967):

$$W^*(x^*,t)=\bar{W}\mathrm{erf}\left(\frac{x^*}{\sqrt{4\nu t}}\right) \tag{8}$$

where erf[•] is the error function and ν is the cinematic viscosity. From a direct inspection of Eq. (8), it follows that the lower is the cinematic viscosity, the sharper is the vertical gust profile at the elapsed time t. In particular, in case of inviscid flow ($\nu = 0$, Re$= \infty$) the vertical gust propagates by pure convection maintaining its initial step profile.
Now let us focus our attention on the computational simulation of the gust, intended here as a perturbation of the mean velocity field. In such a case, two other kinds of viscosity can contribute to smooth the gust profile further. Firstly, if the flow becomes turbulent, the gust is further smoothed by turbulence-induced diffusive effects. For instance, following the Boussinesq hypothesis the additional diffusion is modelled by the so-called turbulent eddy viscosity $\nu_t \propto \mathrm{E}[uw]$, E[•] being the statistical average operator. Secondly, artificial dispersive or diffusive effects can be introduced into the solution because of the discretization procedures in space and time required to transform the

governing set of partial differential equations into an algebraic one. In particular, if a numerical viscosity ν_{num} is superimposed to the cinematic viscosity, the former must be one order of magnitude lower than the latter in order to not overestimate the diffusion of the gust. The above mentioned computational effects mainly depend in FVM on the adopted interpolation scheme, discretisation density and grid quality.

In order to test the spatial discretization, in what follows three upwind schemes are adopted in space discretization for the convection terms in conjunction with orthogonal Cartesian grid uniformly spaced. Their order and leading error term evaluated for the pure convection equation of a generic variable ϕ are summarized in Table 1.

scheme	order	leading error	main effect
UDS	1	$U\Delta x/2\ (\partial^2\phi/\partial x^2)$	diffusive
LUDS	2	$U\Delta x^2/3\ (\partial^3\phi/\partial x^3)$	dispersive
QUICK	3	$U\Delta x^2/24\ (\partial^3\phi/\partial x^3)$	dispersive

Table 1: Interpolation schemes for the convective term.

Because of the dependency of the leading errors to the grid spacing Δx, various Δx are tested. The diffusive term in NSE is approximated using a second order Central Difference Scheme.

Figure 2a shows the spatial profile of the gust simulated at $Re=10^3$ by using $\Delta x=L/160$, L being the dimension of the domain. The results obtained with the above mentioned schemes are compared with the exact solution given by Eq. (8). Coherently with data in Table 1, the diffusive effects introduced by UDS are unacceptable while the LUDS and the QUICK schemes provide a good approximation to the exact solution.

Figures 2b and 2c depict the error ε on the gradient velocity and on the phase difference, respectively, as a function of the space discretization Δx, adopting the three interpolation schemes. The error on the velocity gradient (Figure 2b) using the LUDS and the QUICK schemes are lower than 5% for space discretization $\Delta x< L/160$. The error induced by the UDS scheme decreases more slowly than the other two coherently with its order and diffusive effect (see Table 1). The dispersive effect of both LUDS and QUICK scheme introduces a phase error (Figure 2c), but the one of the LUDS scheme is much greater than the one introduced by the QUICK scheme for $\Delta x< L/320$. Hence, in order to reduce the computational burden, the QUICK scheme is selected because of the moderate numerical dispersion and the very low diffusion introduced even for relatively large $\Delta x/L$.

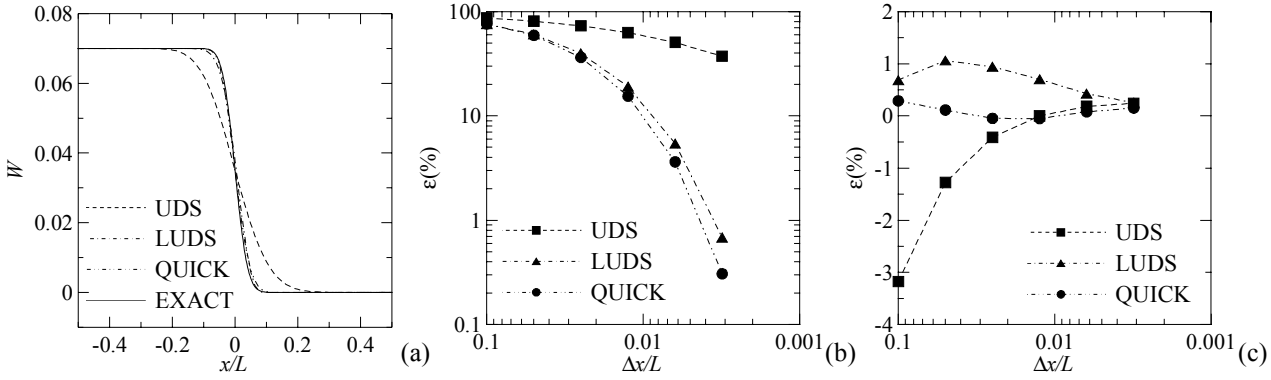

Figure 2: Gust propagation: test of the interpolation schemes for the convection terms.

Once the space interpolation scheme has been chosen and the grid density optimised, the influence of the time step Δt and of the time interpolation scheme are investigated according to Table 2. Moreover, various time steps have been tested.

scheme	order	leading error	main effect
EUL1	1 implicit	$\Delta t/2\ (d^2\phi/dt^2)$	diffusive
EUL2	2 implicit	$\Delta t^2/3\ (d^3\phi/dt^3)$	dispersive

Table 2: Interpolation schemes for the unsteady term.

Figure 3a shows the gust profile obtained with EUL1 and EUL2 schemes at Re=10^3, compared with the exact solution adopting a time step Δt=0.008 expressed in non dimensional time units.
The EUL1 scheme presents unacceptable numerical diffusion, while the EUL2 scheme presents unphysical oscillations for the selected time step, which is not small enough with respect to the characteristic time scale of the gust. Figure 3b shows the error on the velocity gradient for different values of the time step: for Δt=0.002 numerical oscillations are removed and the error of the EUL2 scheme is lower than 5%, while the error due to EUL1 is unacceptable. Hence, in order to maximize the efficiency of the solution, the EUL2 scheme is selected.

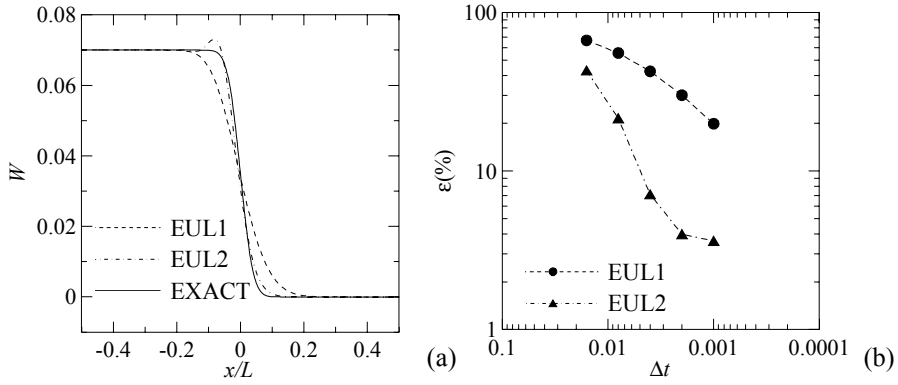

Figure 3: Gust propagation: test of the time interpolation scheme.

It is worthy to observe that the higher is the Reynolds number of the flow, the lower are the diffusive effects due to cinematic viscosity and numerical diffusion is more and more relevant. Thus, the computational simulation of flows characterized by high Reynolds numbers is very sensitive to numerical errors.
A further analysis has been carried out in order to test the accuracy of the numerical solution at Reynolds numbers in the range of interest for Wind Engineering applications, i.e. $10^3 \leq Re \leq 10^6$. Figure 4a compares the exact solution with the numerical ones obtained for a time step Δt=0.001 and a mesh density increased proportionally to Re number adopting as target the same level of accuracy. It emerges that the accuracy of the solution is guaranteed with an acceptable computational burden up to Re<10^5. A further increase of both time and space discretization density would be required to eliminate both the numerical oscillations and the artificial diffusion highlighted at higher Reynolds numbers, involving the unsustainable growth of the computational cost for practical purposes (Figure 4b).

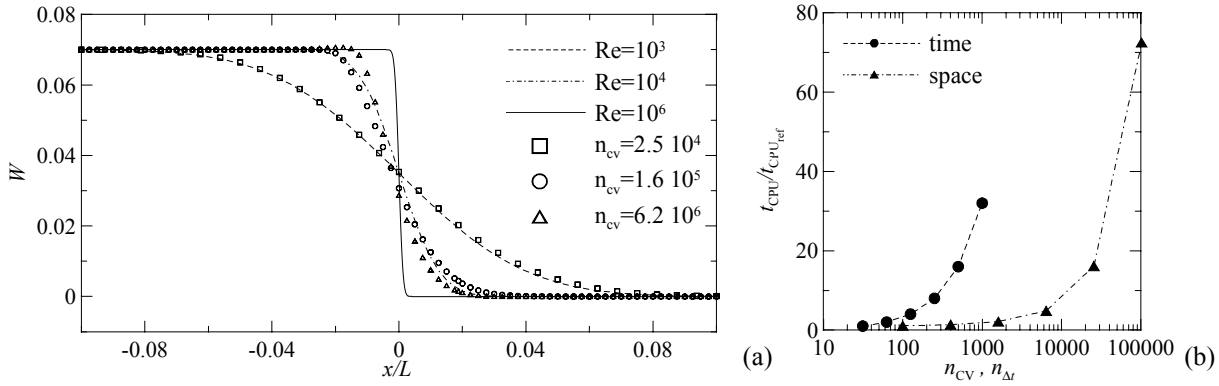

Figure 4: Gust propagation: accuracy of the solution at various Reynolds numbers.

3.2.Steady-state flow past the thin airfoil

The numerical simulation of the steady-state 2-dimensional laminar flow past the thin airfoil with chord B has been carried out considering Re=10^4, Δt=0.001 and a cell thickness close to the wall y_w=0.5 $10^{-5}B$ in order to directly resolve the laminar wall boundary layer. The computational domain extends 15B upwind the plate, 30B downwind and transversally. Figure 5 compares the

numerical solution with the well-known Blasius closed-form one (Batchelor 1967) and with computational results obtained by Walther and Larsen (1997).
The boundary layer profile at x/B=0.5 (Figure 5a), the evolution of the boundary layer thickness δ and the evolution of the friction coefficient C_f along the profile (Figure 5b) are in good agreement with the closed form solution.

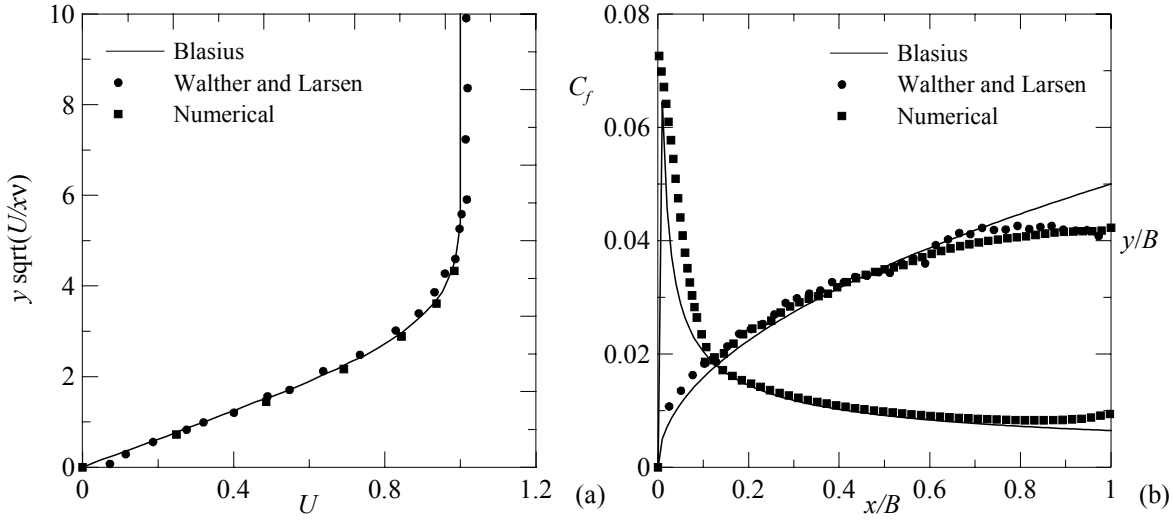

Figure 5: Steady-state flow past the airfoil: boundary layer profile (a), Boundary layer thickness and friction coefficient (b).

4. AIRFOIL RESPONSE TO THE STEP GUST

The gust-generation procedure at the inlet boundary applied in Section 3.1 is hardly extendible to the large computational domains adopted in wall-bounded external flows like the one adopted in Section 3.2. That is mainly due to the computational burden involved by the discretization of the large upwind portion of the spatial domain according to the mesh density requirements discussed above. Further computational cost arises from the discretization of the long time elapsed during the travel of the front of the gust across the upwind sub-domain.
In order to cope with such difficulties, non uniform initial condition are imposed on flow velocity components along the longitudinal axis. The discontinuity is fixed upstream a portion of the upwind sub-domain which includes both the portion of space in which the pressure field is influenced by the obstacle (frontal area) and the one covered by the front of the gust during the time required to dump the unphysical oscillations due to the discontinuity itself (numerical transitory solution). The amplitude of the step variation in transverse velocity component is $\overline{W}$ =8.7 $10^{-3}U$.
The computational tool allows to analyse the flow pattern developing from the interaction between the gust and the thin plate in terms of point and integral quantities. The former can shed some light on the physical phenomena induced by interaction, while the latter will be used to evaluate the aerodynamic admittance function.

4.1. Gust-obstacle interaction

The thin plate immersed in a horizontal flow field is a perfectly streamlined body, so that the aerodynamic forces acting on it are mainly due to the boundary layer surrounding its surfaces. Moreover, the boundary layer is not affected by the null curvature of its surfaces, thus its aerodynamic behaviour is neutral and very sensitive to the perturbations of the incoming flow.
Let us suppose that the gust boundary (defined as the points in xz plane at which $W = \overline{W}/2$) reaches the leading edge at time t_L. Then, a reduced time $\tau = t - t_L$ can be introduced. In Figure 6a the short-term effect of the gust on the airfoil is analysed by observing the evolution in time τ of the boundary layer surrounding the upper surface of the plate. It can be observed that the thickness of the boundary layer locally increases as the gust boundary passes through by effect of the suction of the gust. It follows that the aerodynamic behaviour of the plate is strongly and directly influenced

by a gust of even low intensity. The influence of the obstacle on the gust is studied by observing the evolution in time of the geometry of the gust boundary passing through the domain (Figure 6b). The effects are negligible in the frontal area (straight boundary) because of the small blockage of the obstacle due to its small effective thickness. On the contrary, the gust boundary is deformed in the wake of the obstacle due to the vorticity shed into the wake from the trailing point of the plate when the front gust leaves the obstacle. At following times the vorticity is less concentrated and the extension of the deformed part of the front indicates the instantaneous width of the wake. Finally the boundary is almost straight again when the obstacle perturbation vanishes.

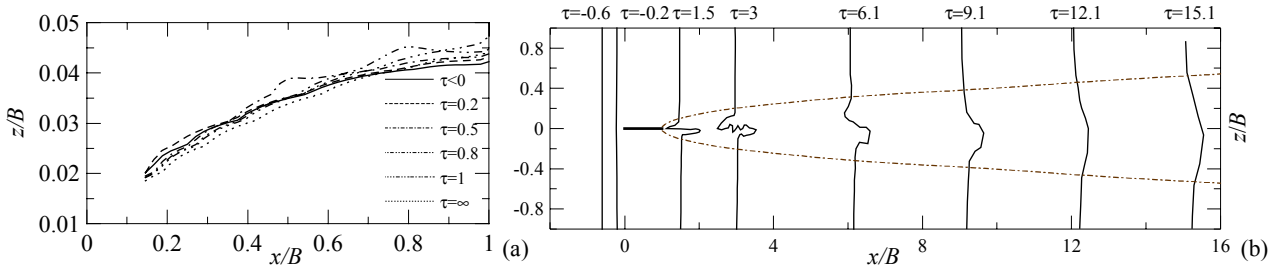

Figure 6: Evolution of the boundary layer (a), evolution of the front of the gust (b)

4.2.Aerodynamic admittance function

As already explained in Section 1, the aerodynamic admittance function is the transfer function of the filter mapping the vertical velocity component into the lift force. The choice of the measure point of the vertical velocity is somewhat arbitrary: a point in the upwind sub-domain, outside the region in which the velocity field is affected by the obstacle but as close as possible to the obstacle is chosen. Analyses have been carried out considering three flow conditions. The inviscid flow is analysed in order to simulate flow conditions as close as possible to potential flow hypothesis and to isolate the effects of pure numerical viscosity. A second simulation in viscous laminar flow is carried out. Finally, a RNG k-ε turbulent model is assumed adding an eddy viscosity in spite of the laminar nature of the boundary layer in order to evaluate the effects of a further increase of the overall viscosity on aerodynamic admittance function. Figure 7 shows the time evolution of the vertical incoming velocity (Figure 7a) and of the normalized lift force (Figure 7b) for the three flow conditions, compared with the Küssner function (Fung 1993). The introduction of the viscosity in the incident flow causes a smoothing of the gust (Figure 7a), which becomes more and more smoothed passing from the inviscid to the viscous to the turbulent incident flow; the effect of the smoothing of the gust profile can be detected in the lift force (Figure 7b).

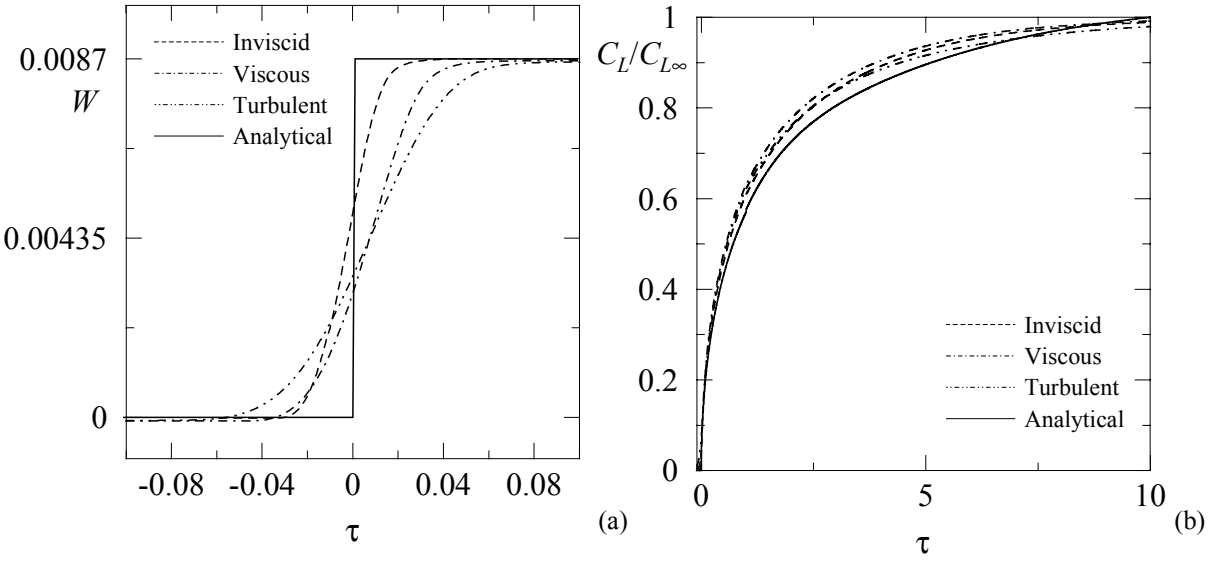

Figure 7: Time evolution of the vertical velocity (a) and of the lift coefficient (b).

Since the time histories of the vertical velocity component $W(\tau)$ and of the lift force $C_L(\tau)$ (Figure 7) are not absolutely integrable and their Fourier transforms cannot be defined, Eq. (4) is used to estimate the aerodynamic admittance function.
Figure 8 shows the time histories of the time derivative of the vertical velocity component (Figure 8a) and of the lift force (Figure 8b). As the velocity component and the lift force (Figure 7) represent a smoothed step function and the airfoil response to a smoothed gust, respectively, their time derivatives represent a smoothed impulse and the response of the airfoil to a smoothed impulse.

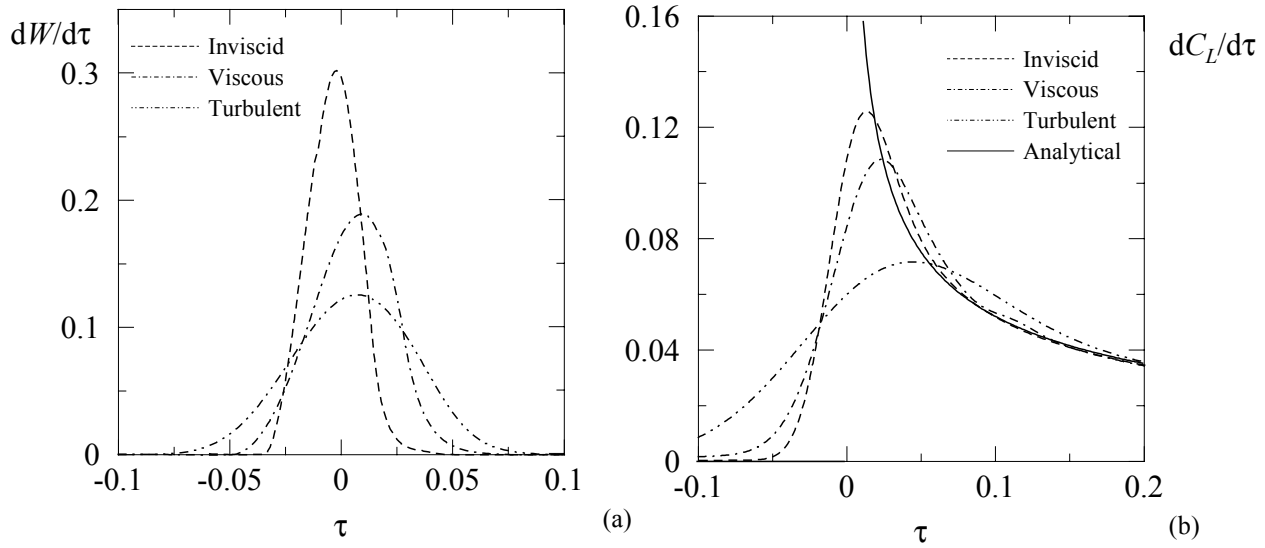

Figure 8: Time histories of the time derivative of the vertical velocity (a) and of the lift coefficient (b).

Figure 9a shows the harmonic content of the time derivative of the vertical velocity component obtained in the three simulations. The input impulse becomes smoother passing from the inviscid flow to the viscous and to the turbulent flow (Figure 8a); thus, the harmonic content is decreased gradually in the high frequency range (Figure 9a). However, the harmonic content of the input is high enough in the frequency range of interest. Figure 9b depicts the aerodynamic admittance functions numerically evaluated in the three flow conditions, compared with the closed form solution (Sears function, Fung 1993). The numerical results obtained for the inviscid and viscous flow conditions are in good agreement with the closed form solution. The aerodynamic admittance function evaluated for the turbulent condition is lower than the theoretical one in the range of high reduced frequencies. This difference is due to the introduction of an eddy viscosity model, which acts like a low pass filter.

5. CONCLUSIONS

The present paper discusses the possibility of estimating the aerodynamic admittance function for a thin airfoil through the computational simulation of the propagation of a sharp-edge gust.
The computational approach required to obtain the accurate simulation of the physics of the flow of interest is assessed. The computational tool has proved to be very efficient for Reynolds number equal or lower than 10^4. The cost of the computational simulation rapidly increases for higher Reynolds numbers since a finer discretization is required both in space and in time.
The classical indicial approach is modified in order to guarantee its compatibility with the computational tool and to allow its application for viscous flows. Thanks to the post processing facilities of the computational tool, the proposed approach allows the physical interpretation of the interaction between the gust and the obstacle. Moreover, the obtained results are in good agreement with analytical solutions present in literature. The possibility of applying the method to bluff bodies in different flow conditions is investigated in a companion paper (Bruno *et al* 2004).

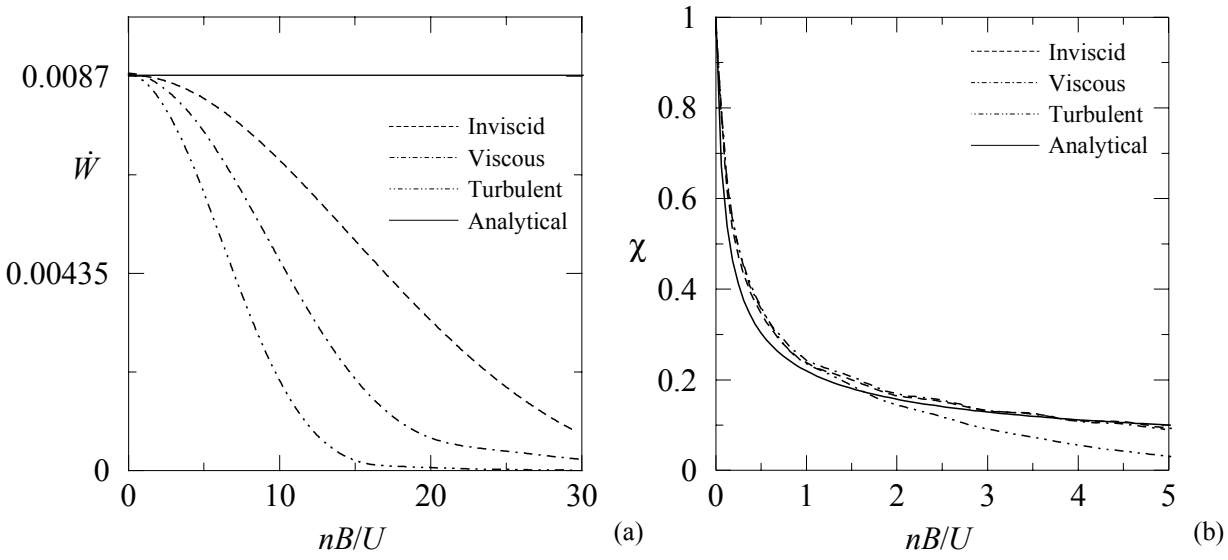

Figure 9: Harmonic content of the time derivative of the vertical velocity (a) and aerodynamic admittance function (b).

6. ACKNOWLEDGMENTS

The authors wish to express their grateful acknowledgment to the L3M - Laboratoire de Modélisation et Simulation Numérique en Mécanique – Marseille - France for the kind availability of the computing facilities.

7. REFERENCES

Ballhaus W.F., Goorjian P.M. (1978), Computation o unsteady transonic flow by the indicial method, *AIAA Journal*, Vol. 16(2).

Batchelor G.K. (1967), *An introduction to Fluid Dynamics*, Cambridge University Press, Cambridge.

Bruno L., Tubino F. and Solari G. (2004), Aerodynamic admittance functions of bridge deck sections by CWE, *Proceedings 8th Italian National Conference on Wind Engineering*, Reggio Calabria, Italy.

Cigada A., Diana G., Zappa E. (2002), On the response of a bridge deck to turbulent wind: a new approach, *J. Wind Engng and Ind. Aerodynamics*, Vol. 90, pp. 1173-1182.

Fung Y.C. (1993), *An introduction to the theory of aeroelasticity*, Dover Publications, New York, U.S.A.

Larose G.L. (1999), Experimental determination of the aerodynamic admittance of a bridge deck section, *J. Fluids and Structures*, Vol. 13, pp. 1029-1040.

Lesieutre D.J., Reisenthel P.H., Dillenius M.F.E. (1994), A pratical approach for calculating Aerodynamic indicial functions with a Navier-Stokes solver, AIAA 94-0059, *32nd Aerospace Sciences Meeting & Exhibit*.

Murakami, S., Iizuka, S., Tsuchiya, N., Mochida, A. (1999), LES of flow past 2D cylinder with imposed inflow turbulence, *Proceedings 10th International Conference on Wind Engineering*, Balkema, Rotterdam, pp. 1291-1298.

Parameswaran V., Baeder J.D. (1997), Indicial Aerodynamics in Compressible flow – Direct calculations, *AIAA J. Aircraft*, Vol. 34, pp. 131-133.

Tamura T. (1990), On the reliability of two-dimensional simulation for unsteady flows around a cylinder-type structure, *J. Wind Eng. Ind. Aerodyn.*, Vol. 35, pp. 275-298.

Turbelin G. (2000), *Modélisation de la turbulence atmosphérique en vue de l'étude du chargement aérodynamique des structures soumises aux effets du vent*, PhD Thesis, Université d'Evry Val d'Essonne, France.

Von Karman T. and Sears W.R. (1938), Airfoil Theory for Non-Uniform Motion, *Journal of Aeronautical Science*, Vol. 10(5).

Walther J.H., Larsen A. (1997), Two dimensional discrete vortex method for application to bluff body aerodynamics, *J. Wind Engng and Ind. Aerodynamics,* Vol. 67-68, pp.183-193.